ELSEVIER

Polymer 41 (2000) 8975–8981

polymer

www.elsevier.nl/locate/polymer

Real-time crystallization study of poly(ϵ-caprolactone) by hot-stage atomic force microscopy

L.G.M. Beekmans, G.J. Vancso*

Faculty of Chemical Technology and MESA+ Research Institute, University of Twente, P.O. Box 217, 7500 AE Enschede, The Netherlands

Received 25 October 1999; received in revised form 3 February 2000; accepted 10 February 2000

Abstract

The morphological development and lamellar growth kinetics of poly(ϵ-caprolactone) (PCL) were investigated in real-time by hot-stage atomic force microscopy (AFM). The morphology of PCL crystals grown in the melt was studied to obtain insight into the mechanism, which controls the lateral shape of the lamellae in this polymer. Melt-grown PCL crystals showed a truncated lozenge lateral shape, with curved or chair-like three-dimensional morphology. Similar lamellar morphologies were observed in larger crystal aggregates, i.e. hedrites, grown at lower crystallization temperatures in the melt. The individual lamellae in these crystal aggregates also showed an elongated truncated lozenge shape. The AFM examination of the hedritic morphologies revealed the dynamics of the dominant/subsidiary crystallization process. The use of a hot-stage allowed us to perform real-time observation of growth faces in different crystallographic directions. The results support previous evidence, which suggested that the elongated lamellar habit is related to growth rate anisotropy. Morphological observations suggest a mechanism including {110} growth faces. In addition, visualization of the lamellar morphology indicates that the PCL crystals are obtained under regime II crystallization conditions.

Keywords: Poly(ϵ-caprolactone); Crystallization; Morphology

1. Introduction

Spherulitic textures are among the most commonly observed morphologies in semi-crystalline polymers. The generation of a spherulite starts from a precursor structure, which quite often consists of a lamellar crystal. This precursor then develops into a spherically symmetric structural entity. The detailed description of the lamellar organization within the spherulite, as well as the lateral habit of the individual lamella, has been the subject of intensive studies [1–7]. Historically, electron microscopy (EM) has afforded remarkable insight into the structure of semi-crystalline polymers. Based on EM observations, Vaughan, Bassett, and coworkers have identified the basic steps in the development of spherulitic morphology [2]. The first step involves the formation of dominant lamellae, which form a three-dimensional skeleton by splaying and branching. In a subsequent step, subsidiary lamellae fill-in the structure between the dominant lamellae.

The first mechanism to describe the development of the lateral shape of the lamellae in polymer crystals was proposed by Keith and Padden based on optical microscopy (OM) observations [3]. They proposed that polymer spherulites consist of ribbon-like, highly elongated lamellae separated by layers of uncrystallized melt. The elongated habit results from the diffusional segregation of impurities of low molar mass material at the growth fronts. Keith and Padden later recognized that in the case of polymers, in which the unit cell exhibits a two fold rotational symmetry around the chain axes, elongated lamellae could result from an anisotropy in growth rates [5]. The basic growth habit of polyethylene (PE) lamellar crystals is indeed elongated in the radial direction when grown from the melt or solution at high crystallization temperatures [2,4,6,7].

The application of scanning probe microscopy to polymer systems is gaining wide acceptance as a complementary technique to EM or OM in polymer crystallization studies. It has been shown that atomic force microscopy (AFM) images can be obtained on polymer crystals with molecular lattice resolution [8–10]. Single crystals [11], as well as melt-crystallized polymers [11–13] were also studied. Despite the many insights into polymer morphology gleaned by using EM and AFM, these techniques have hitherto proven useful mostly for static measurements. In the case of semi-crystalline polymers, such studies require the growth of polymer crystals (single crystals or larger

* Corresponding author. Tel.: +31-53-489-29-74; fax: +31-53-489-38-23.

E-mail address: g.j.vancso@ct.utwente.nl (G.J. Vancso).

0032-3861/00/$ - see front matter
PII: S0032-3861(00)00240-8

complex crystal aggregates) followed by quenching to room temperature and, in a subsequent step, transfer to the electron microscope or AFM for examination. Most dynamic, hot-stage studies of morphological development in situ have been performed using OM, with its limited resolution.

The ability of AFM to follow real-time dynamics of processes, albeit with some limitations in speed, is now established. One of the first reported examples is the real-time AFM study by Drake and coworkers on clotting of blood protein [14]. The morphological changes and growth in polymer crystals were also reported [15–17]. In the context of polymer morphology, the application of AFM to dynamic processes was restricted to ambient temperatures until recently. The development of heating devices has extended the utility of in situ AFM for study of melting transitions in Langmuir–Blodgett films [18]. Recently, our group reported real-time AFM studies on the melting and crystallization in poly(ethylene oxide) (PEO) and PEO/atactic poly(methyl methacrylate) blends at elevated temperatures [19–22]. An independent AFM melt crystallization study of PEO was also published in which the use of tapping mode AFM (TM-AFM) at elevated temperatures was demonstrated [23].

Both contact and tapping mode AFM are used to observe the lamellar habit in PCL at the crystallization temperatures in real-time. In contact mode AFM the tip is raster scanned in contact with the sample surface. In tapping mode AFM, the sample surface is probed by an oscillating tip-cantilever. The tip contacts the surface in each cycle of its vibration thereby minimizing the shear forces acting on the surface as compared to contact mode AFM [24]. As an extension to normal tapping mode, phase imaging was applied to obtain a sharp contrast between the features imaged. Phase contrast provides a map of stiffness variation [25] at the surface and is able to resolved melt crystallization on a lamellar scale [22]. The images resemble micrographs that can be observed in transmission electron microscopy (TEM) images of etched and replicated sample surfaces.

In this paper, we report on results of an investigation of the morphology of melt-grown crystal lamellae of poly (ϵ-caprolactone) (PCL) by a real-time hot-stage AFM study. PCL was chosen for this study because of its low equilibrium melting temperature of 70°C. Although our custom built hot-stages allow for imaging at present up to approximately 150°C, the relatively low melting temperature is convenient for practical experimental reasons. Whereas previous PCL morphology studies were limited to investigations with electron microscopy [26–28] and AFM [28–30] of fully crystallized samples, they do not provide insight into the mechanism of crystallization. Quenching of PCL ($T_g = -71$°C), which allows one to perform static measurements at room temperature, results in a two-step crystallization process with corresponding highly complex crystal morphologies. It is anticipated that a real-time crystallization study of PCL by AFM with lamellar resolution shall provide new insight into the organization of the lamellae within melt-crystallized spherulites of this polymer.

In addition, PCL is very similar to PE in a structural sense since its unit cell resembles closely that of PE [31,32]. The unit cell of PCL is different in the *c* direction as compared to PE due to the ester linkage in the polymer chain. Traditionally, melt crystallization studies have been focused on materials with a minimum degree of complexity such as PE. Detailed investigations have been made of the morphology of PE, which is one of the best-characterized semi-crystalline polymers [1–7].

2. Experimental

2.1. Materials

PCL with a molar mass of 55×10^3 g/mol was obtained from Aldrich. The polymer was purified by precipitation from a chloroform solution-using methanol as the nonsolvent. Samples were prepared by casting from dilute (ca. 3%) chloroform solution on cleaned glass slides at 50°C. The samples were first dried in air at 50°C overnight and then dried in vacuum for 1 day at room temperature. The heating stage used for contact mode AFM observations is described elsewhere [19–21], while in tapping mode investigations heating was performed using a Peltier element [22]. The temperature was calibrated using a small disk K-type thermocouple, and checked using compounds of known melting points (benzophenone, 99% and chlorobenzophenone, 99%). Isothermal crystallization experiments were performed by heating the samples in the AFM apparatus to approximately 100°C for 10 min, and then quenched to the desired crystallization temperatures. For the PCL lamellar crystal experiments the temperature at which the samples were melted prior to crystallization was lowered to 72°C.

2.2. Atomic force microscopy

AFM experiments were performed on a NanoScope III setup (Digital Instruments). The instrument was equiped with a J-scanner (maximum scan size 100 μm^2) which was calibrated in *x*- and *y*- directions by using samples of microcontact printed self-assembled monolayers of different thiols (OH and CH_3 terminated) on a gold substrate [33] with known pattern characteristics. The *x*- and *y*- directions of the scanner were stable over the entire temperature range as used in this study. AFM images were obtained in air while operating the instrument in the contact or tapping mode. Commercially available Si_3N_4-cantilevers were used with force constants of 0.38 N/m as stated by the manufacturer for contact mode measurements and Si-cantilevers with force constants of 27–83 N/m for tapping mode. Measurements in contact mode were carried out with minimized imaging forces. Height and deflection or height and phase images are acquired simultaneously using contact or tapping mode, respectively.

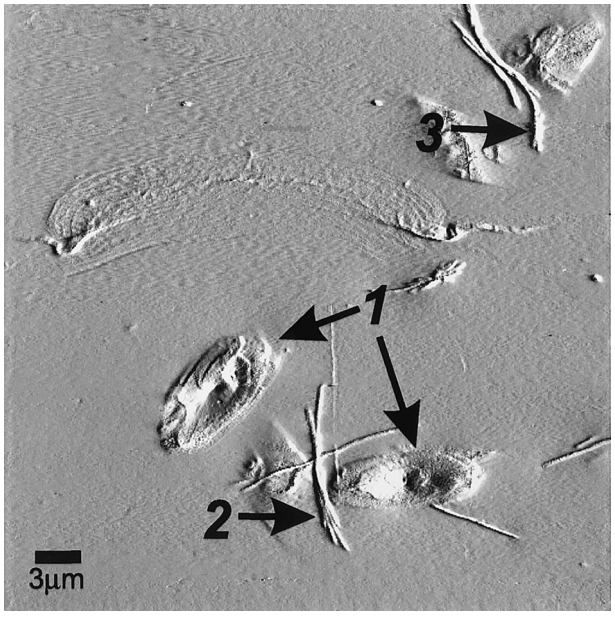

Fig. 1. AFM contact mode, deflection image of PCL single crystals after 24 h of growth at 62°C. The crystals indicated by (*1*) correspond to flat-on crystal views while (*2*) and (*3*) correspond to edge-on views.

3. Results and discussion

3.1. PCL lamellar crystals

We first focused on an examination of the crystalline development at a lamellar crystal level. Isolated lamellar crystals were initially selected because of the relatively simple morphology. The crystals provide the basis for the lamellar habit in melt-grown PCL crystal aggregates. Lamellar crystals are observed when the crystallization is performed at relatively low degrees of undercooling. Fig. 1 shows PCL lamellar crystals which were melt-crystallized at a temperature of approximately 62°C. The image was acquired in contact mode AFM at the crystallization temperature. The basic growth habit of the PCL lamellar crystals is the truncated lozenge shaped lateral habit with curved edges (type *1*, flat-on view). The edge-on crystal projections exhibit curved (type *2*) and chair-like (type *3*) three-dimensional shapes. The observations of smaller PCL crystals with planar habit correspond to a projection further from the center of the lamellar crystal.

It is interesting to note that similar crystals have been reported for PE crystallized from the melt in very thin films [6,7] or solution [4] at relatively high crystallization temperatures. The main characteristics of the PE crystals were the elongated lateral habit and the curved growth faces. Two different types of melt-grown lamellar crystals were identified for PE exhibiting planar elliptic [2] and truncated lozenge shapes [7]. Planar lenticular PE single crystals with curved faces extending toward the apex of the lamellae under an acute angle are obtained under regime I crystallization conditions. At higher undercooling (regime II), there was a transition to crystals with a truncated lozenge shape with a chair-like/curved three-dimensional morphology [6]. Similarly to PE in regime II, the main characteristics of the PCL lamellar crystals includes curved growth faces with an apex angle $\alpha > 90^\circ$ (type *1*; the angle α, as defined in Fig. 3C, is discussed in more detail in Section 3.2) and the crystals exhibit a chair-like/curved three-dimensional shape (types *2* and *3*). The PCL morphology indicates that the lamellar crystals shown in this study were grown under regime II crystallization conditions.

Phillips and co-workers [26] suggested a regime II growth for PCL in the temperature range from 39 to 51°C, based on a crystallization kinetics study of spherulitic growth rates as observed by OM. Moreover, in a similar study by Chen and co-workers [34], it was suggested that the growth of PCL in the temperature range above 35°C up to 43°C was located in regime II independent of molar mass. A transition in growth regimes (II–I) was not observed in these PCL crystallization studies [26,34]. The morphological evidence in the present study suggest regime II controlled growth for the PCL crystals ($M_n = 55 \times 10^3$ g/mol) up to 62°C.

The different appearances of the crystals in the image of Fig. 1 are explained by different cross-sections of lamellar crystals observed at the imaged surface. The crystals are nucleated at various depths below the surface and are randomly oriented. The area of a given crystal that intersects the surface is consequently also random. Our AFM experiments, therefore, captured various view directions and different levels of intersection of the PCL crystals.

Although it is possible to image morphologies on a lamellar scale by contact mode AFM [19–21], tip induced crystallization by shear forces makes direct real-time observations of the crystallization process in the case of PCL difficult [22]. To eliminate the uncertainties associated with this tip-induced crystallization the study was extended to tapping mode AFM (TM-AFM) [24,25].

3.2. PCL crystal aggregates

In searching further for the factors that contribute to the mechanism of lamellar development, our examination concentrated on PCL crystal lamellae found in a relatively advanced state of crystalline development that more closely approached the complexity of lamellar organization of melt-crystallized spherulites. Hedritic crystalline morphologies can be obtained under faster crystallization kinetics, a condition that is experimentally created by higher undercooling. As shown in Fig. 2, hedrites with a high degree of complexity were obtained from the melt upon lowering the temperature of crystallization to approximately 56°C. Fig. 2 contains a series of phase images of a PCL hedrite acquired in tapping mode AFM at different time intervals. Clearly visible in the successive images is the absence of any tip-induced crystallization process [22]. No solidification of

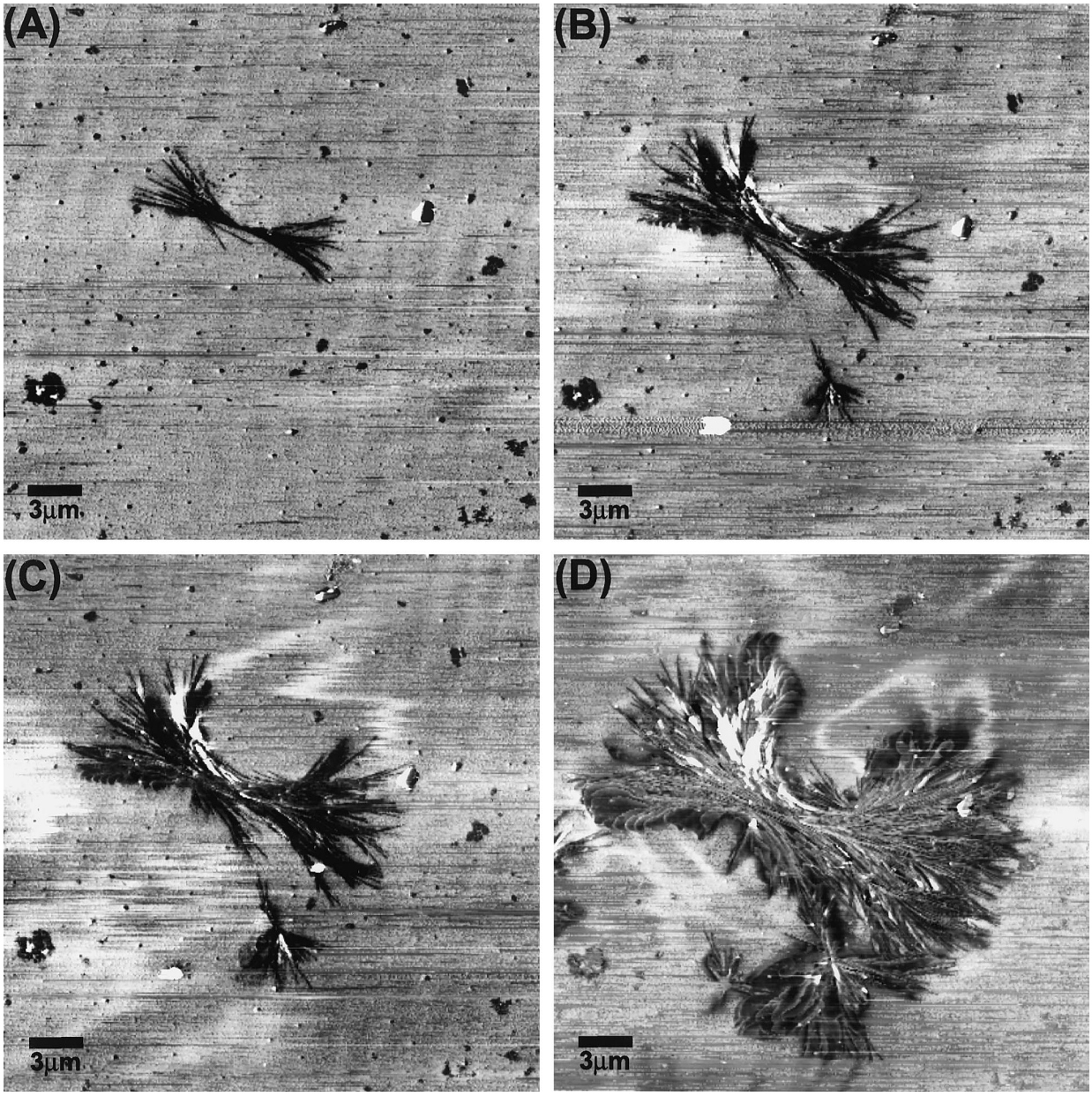

Fig. 2. (A–D) AFM phase images of PCL hedrite growing at 56°C; the images in (B), (C), and (D) correspond to elapsed times of 244 min, 290 min, and 551 min, respectively, with respect to the image in (A).

the surrounding unperturbed melt took place up to at least 550 min (Fig. 2D) after which imaging was stopped.

The projection seen in Fig. 2 corresponds to an edge-on view near the center of the hedrite. Observation of slightly different lamellar projections (closer to flat-on), more pronounced in Fig. 2C and D, indicate a tilt of the crystal with respect to the surface. The morphological development comprises at first the formation of a skeleton of dominant lamellae. This is clearly visible in the initial stage of crystallization as seen in the image of Fig. 2A. The structure consists of lamellae of approximately equal lateral dimensions separated by melt. The onset of branching is also seen in Fig. 2A. The lamellae developing in this subsequent step are named subsidiary, which diverge, thus filling the skeleton. The dynamics of this space filling can clearly be observed in the next images. The subsidiary lamellae originating from the edge of the skeleton eventually develop a dominant character. The change in dominance is governed by the lamellar surrounding and will eventually yield to the development of the characteristic eyelets as observed in the interior of most polymeric spherulites. The series of images shown in Fig. 2 is unique in reporting for the first time direct observations of the successive stages in the development of PCL hedrites as depicted until now only in the schematic representations of Ref. [1] (p 468, stages 2–4, edge-on view).

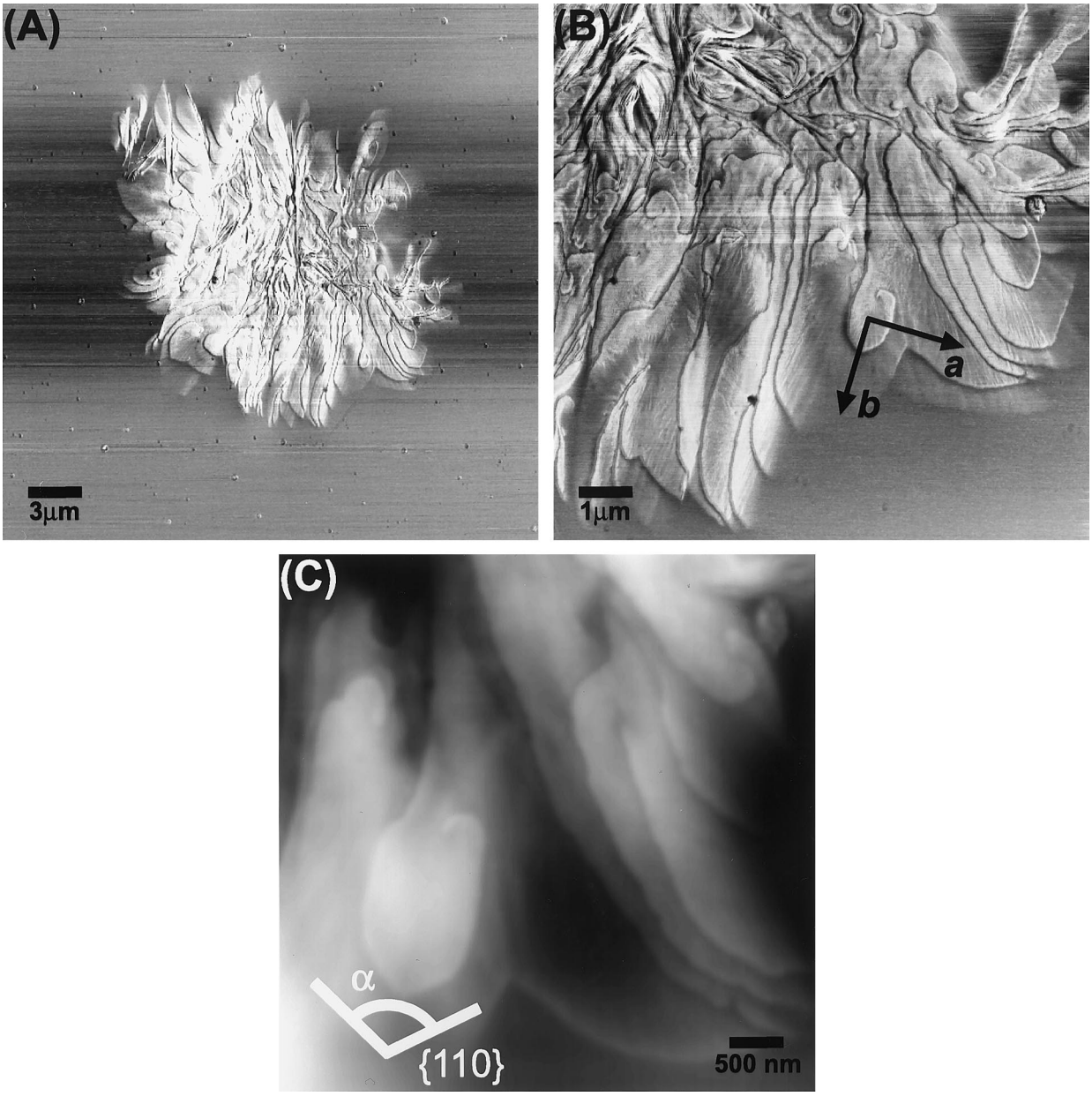

Fig. 3. (A and B) AFM phase images of PCL hedrite growing at 57°C; the image in (B) was obtained at higher magnification and corresponds to an elapsed time of 33 min with respect to the image in (A). (C) AFM height image corresponding to an elapsed time of 67 min, with respect to the image in (A). The vertical scale in (C) is 400 nm (dark to bright).

In view of the previous section our study was then directed to the characteristic habit of the individual lamellae. In Fig. 3A is seen a phase image of a PCL hedrite growing at a temperature of 57°C. Noteworthy are the different orientations of the individual lamellae. The images in Fig. 3B and C show a higher magnification phase and height images of lower right part of the hedrite. The lamellae indicated by the crystallographic *a* and *b* axes in Fig. 3B grows parallel to the surface which corresponds to a flat-on view as it was confirmed by the height images, for example in Fig. 3C. The former height image has poorer lateral resolution but allows for a characterization of the actual height. This, and similar, flat-on views allow for unambiguous observation by AFM of the lamellar habit and its development in time. The lamellar morphology corresponds to a truncated lozenge shape with curved edges, similar to the PCL lamellar crystals shown in Fig. 1.

Although the crystal structure of PCL is established [31,32], there is no direct information on the growth front. An electron diffraction study of solution-grown PCL lamellar crystals indicated {110} and {200} growth faces [32]. It is perhaps not a coincidence that similar growth faces were identified in PE melt-grown lamellae. Evidence for the {110} growth faces was sought for by analyzing the apex angle (α), as defined in Fig. 3C. The value of α was measured from truncated crystals with straight {110} faces

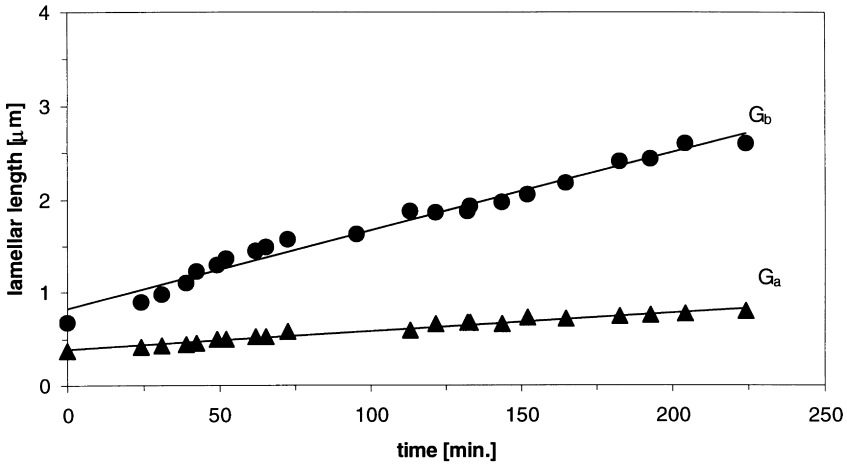

Fig. 4. Lamellar length along the *a* (▲) and *b* (●) axes as a function of time at 57°C.

in the radial direction. It should be pointed out that the analysis was restricted to lamellae that were growing parallel to the surface since a distinct angle between the axial *a* axes of the crystal and the imaged surface would result in an underestimate. A further restriction upon the crystal population studied was imposed by the presence of the surface. Only lamellae with linear growth rate in radial direction, as discussed in the next paragraph, were considered to be representative. An average value of $110 \pm 2^{\circ}$ was eventually estimated for the value which agrees to within experimental error with corresponding values obtained previously in EM studies of PE [4] and PCL [32] single crystals. It is therefore expected that the lamellar crystals are bounded by {110} faces with truncating {200} faces. The corresponding crystallographic axes are shown schematically in Fig. 3B.

The series of phase images shown in Fig. 3 contains information on the growth rates of the faces. The growth rates are estimated for the crystallographic *a* and *b* axes, G_a and G_b, respectively. The directional length versus time data is shown in Fig. 4, from which linear growth rates were estimated for the different crystallographic axis. The growth rates were measured by using screw dislocations as fixed reference points. Table 1 summarizes the average growth rates that were estimated for the {200} and {110} growth faces of different flat-on seen lamellae ($G_{\{110\}} = G_b \sin(\alpha/2)$, $G_{\{200\}} = G_a$). For comparison, the growth rates of edge-on seen lamellae were also estimated at the same crystallization temperature ($G_{edge,b,}$ Table 1). It seems that $G_{edge,b}$ is in agreement with the kinetic data obtained for the {110} growth faces ($G_{\{110\}}$) taking in to account the value of α. Some disagreement with the radial growth rate $G_b = 7.0 \pm 1.1$ nm/min and $G_{edge,b}$ is expected since it is experienced that the PCL crystals are randomly oriented and only the projection of the edge is captured. A distinct angle between the radial *b* axes of an edge-on growing lamella and the imaged surface results in an underestimate of its growth rate. The higher growth rate for the *b* direction in flat-on projections (G_b) suggests that the influence of the surface on the crystallization process is negligible. In the case of flat-on seen lamellae growing parallel to the surface, the crystal growth is constrained in two-dimensions: by the melt/air interface and by the underlying lamellae, as compared to edge-on seen lamellae. This observation of $G_{edge,b} < G_b$ seems wider implacable since it suggests that growth rates measured by OM in films of restricted dimensions, semi two-dimensionally, are representative for the growth rate in the bulk (three-dimensional).

Table 1
Averaged lamellar growth rates for PCL at different crystallization temperatures (values are obtained by averaging over at least 4 individual measurements and the errors represent the standard errors of the population)

Temperature (°C)	$G_{edge,b}$ (nm/min)	*G* flat-on (nm/min)	
		$G_{\{110\}}$	$G_{\{200\}}$
57	5.9 ± 0.8	5.7 ± 0.9	1.9 ± 0.1

It is of interest that the growth faces of the individual PCL lamellae display differences in growth rate. A three-fold difference is observed between $G_{\{110\}}$ and $G_{\{200\}}$, which is related to the crystal structure, i.e. the two fold rotational symmetry around the chain axes. In the case of polymers with low crystallographic symmetry, the radial elongated lamellar habit, which is often observed in spherulites, seems to results from this anisotropy in growth rates [5]. This is consistent with the available data for solution-grown PE lamellar crystals [4]. Whereas later PE single crystal crystallization studies confirmed this anisotropy in growth rates, morphological observations were limited to static electron microscopy measurements [6,7]. Linear growth rates were estimated from the lateral size of the single crystals at the time of sampling. Axial ratios ($G_b/G_{\{200\}}$) of 1.0–2.6 were reported for PE crystallized from the melt in regime II [6] or crystallized from dilute solution [4]. The PCL lamella growing at 57°C exhibit a relatively higher axial ratio of 3.5. Compared to PE, the introduction of an

ester linkage, which are somewhat aligned in the crystallographic a direction [31,32], seems to increase the anisotropy between the growth faces in PCL crystals.

4. Summary and conclusions

The present study of the morphology of PCL crystals grown from the melt shows that the native rhombic habit of the lamellae is elongated which indicates an anisotropy in growth rates for different crystallographic directions. The observed lamellar crystal morphology is identified as truncated lozenges with a three-dimensional chair-like or curved shape and suggests that the PCL crystal growth was located in regime II for the different crystallization temperatures employed in this study. The examination of lamellar morphology in larger crystal aggregates by TM-AFM is consistent with our static high temperature contact mode AFM observation. Experimental evidence obtained indicates {110} growth faces in the radial direction of the PCL crystals. The dynamic process of polymer crystallization by dominant and subsidiary lamellae in PCL was visualized. The lamellar lateral habit development was monitored and the growth rates for the crystallographic directions were estimated. The interesting morphological characteristic observed in the large aggregates was the anisotropy in linear growth rates for the different growth faces, obtained to our knowledge for the first time by direct AFM observations. The kinetic results indicate that the crystallization process is not influenced by the presence of a polymer melt/air interface.

Acknowledgements

The authors are grateful to the Dutch Foundation for Chemical Research (NWO-CW) for financial support and to Dr D.L. Trifonova (University of Twente) and Dr R. Pearce (Barringer Research) for helpful discussions.

References

[1] Khoury F, Passaglia E. In: Hannay NB, editor. Treatise on solid state chemistry, vol. 3. Plenum Press: New York, 1976.
[2] Vaughan AS, Bassett DC. In: Booth C, Price C, editors. Comprehensive polymer science, vol. 2. Oxford: Pergamon Press, 1989.
[3] Keith HD, Padden Jr. FJ. J Appl Phys 1963;34:2409.
[4] Organ SJ, Keller A. J Mater Sci 1985;20:1571.
[5] Keith HD, Padden Jr FJ. Polymer 1986;27:1463.
[6] Toda A. Colloid Polym Sci 1992;270:667.
[7] Toda A, Keller A. Colloid Polym Sci 1993;271:328.
[8] Stocker W, Magonov SN, Cantow HJ, Wittmann JC, Lotz B. Macromolecules 1993;26:5915.
[9] Snétivy D, Vancso GJ. Polymer 1994;35:461.
[10] Stocker W, Schumacher M, Graff S, Thierry A, Wittmann JC, Lotz B. Macromolecules 1998;31:807.
[11] Vancso GJ, Nisman R, Snétivy D, Schönherr H, Smith P, Ng C, Yang H. Colloids Surf, A, Phys and Engng Asp 1994;87:263.
[12] Singfield KL, Klass JM, Brown GR. Macromolecules 1995;28:8006.
[13] Schönherr H, Snétivy D, Vancso GJ. Polym Bull 1993;30:567.
[14] Drake B, Prater CB, Weissenhorn AL, Gloud SAC, Albrecht TR, Quate CF, Cannell DS, Hansma HG, Hansma PK. Science 1989;243:1586.
[15] Harron HR, Pritchard RG, Cope BC, Goddard DT. J Polym Sci: Part B Polym Phys Ed 1996;34:173.
[16] Hobbs JK, McMaster TJ, Miles MJ, Barham PJ. Polymer 1998;39:2437.
[17] Ivanov DA, Jonas AM. Macromolecules 1998;31:4546.
[18] Sikes HD, Schwartz DK. Science 1997;278:1604.
[19] Pearce R, Vancso GJ. Macromolecules 1997;30:5843.
[20] Pearce R, Vancso GJ. Polymer 1998;39:1237.
[21] Pearce R, Vancso GJ. J Polym Sci: Part B Polym Phys Ed 1998;36:2643.
[22] Vancso GJ, Beekmans LGM, Trifonova D, Varga J. J Macromol Sci: Part B Phys 1999;38:491.
[23] Schultz JM, Miles MJ. J Polym Sci: Part B Polym Phys Ed 1998;36:2311.
[24] Carpick RW, Agraït N, Ogletree DF, Salmeron M. Langmuir 1996;12:3334.
[25] Bar G, Thomann Y, Brandsch R, Cantow H-J. Langmuir 1997;13:3807.
[26] Phillips PJ, Rensch GJ, Taylor KD. J Polym Sci: Part B Polym Phys Ed 1987;25:1725.
[27] Keith HD, Padden Jr FJ, Russell TP. Macromolecules 1989;22:666.
[28] Wang C, Kressler J, Thomann Y, Cramer K, Stuhn B, Svoboda P, Inoue T. Acta Polym 1997;48:354.
[29] Lee J-C, Nakajima K, Ikehara T, Nishi T. J Appl Polym Sci 1997;64:797.
[30] Kressler J, Wang C, Kammer HW. Langmuir 1997;13:4407.
[31] Chatani Y, Okita Y, Tadokoro H, Yamashita Y. Polym J 1970;1:555.
[32] Brisse F, Marchessault RH. In: French AD, Garder KH, editors. Fiber diffraction methods, ACS Symposium Series No 141, Washington, DC: American Chemical Society, 1980. p. 273–7.
[33] Kumar A, Biebuyck H, Whitesides GM. Langmuir 1994;10:1498.
[34] Chen H-L, Li L-J, Ou-Yang W-C, Hwang JC, Wang W-Y. Macromolecules 1997;30:1718.